Analytical and Numerical Solutions for Nonlinear Equations
©Available online at https://ansne.du.ac.ir/
Online ISSN: 3060–785X
2024, Volume 9, Issue 2, pp. 203–220
Research article

Efficient Numerical Approximation of Distributed-Order Fractional PDEs Using GL1-2 Time Discretization and Second-Order Riesz Operators

MohammadHossein Derakhshan[1,*], Yadollah Ordokhani[1]

[1] Department of Mathematics, Faculty of Mathematical Sciences, Alzahra University, Tehran, Iran

* **Corresponding author(s):** m.derakhshan@alzahra.ac.ir; M.h.derakhshan.20@gmail.com

Received: 19/08/2025 **Revised:** 12/09/2025 **Accepted:** 30/09/2025 **Published:** 01/10/2025 10.22128/ansne.2025.3022.1147

Abstract

This paper presents a novel and efficient fully discrete numerical scheme for distributed-order fractional partial differential equations involving both the Caputo time-fractional derivative and the Riesz space-fractional derivative. Such equations frequently arise in the modeling of anomalous diffusion and transport phenomena, where accurate and stable computational methods are crucial. The temporal discretization is carried out using the second-order generalized L1 (gL1-2) scheme, which improves accuracy over traditional L1-based methods. For the spatial discretization, the Riesz derivative is approximated by a second-order finite-difference method, ensuring robustness and precision. The resulting scheme provides a high-order numerical framework that can effectively address a wide class of distributed-order fractional models. A rigorous theoretical analysis is conducted, proving unconditional stability and optimal convergence rates via the energy method. The effectiveness of the scheme is further validated through two numerical experiments, which confirm the theoretical results and highlight the computational efficiency, accuracy, and practical applicability of the proposed approach.

Keywords: Distributed-order fractional partial differential equation, Riesz fractional derivative, GL1-2 scheme, Stability analysis

Mathematics Subject Classification (2020): 35R11, 65M06, 65M12, 65M15, 65M70

1 Introduction

In recent years, fractional-order models have emerged as powerful tools for describing complex physical and engineering systems characterized by memory effects, anomalous diffusion, and spatial heterogeneity. Among these models, distributed-order fractional differential equations have gained significant attention due to their enhanced flexibility and ability to capture a wide spectrum of dynamic behaviors [1, 2, 4, 7, 12–14, 24, 25, 27, 29, 31, 35, 38, 39]. Instead of relying on a single fixed order, the distributed-order approach integrates over a range of fractional orders, making it especially suitable for multi-scale and heterogeneous media. The choice of the Caputo fractional derivative in the time direction stems from its natural incorporation of classical initial conditions and its widespread applicability in modeling viscoelastic and diffusive systems. On the spatial side, the Riesz fractional derivative serves as a symmetric, nonlocal operator capable of describing anomalous spatial diffusion more accurately than classical Laplacians. Moreover, the inclusion of a nonlinear term and a Fredholm integral operator of the first kind allows the model to encapsulate complex interactions and integral memory effects often encountered in porous media, population dynamics, or neural field models. The resulting equation is not only mathematically rich but also capable of capturing a wide variety of physical phenomena across disciplines.

We consider the following distributed-order timespace fractional partial differential equation:

$$\int_0^1 \omega(\alpha)\, {}^C D_t^{\alpha} u(x,t)\, d\alpha = \int_0^2 \rho(\beta)\, (-\Delta)^{\beta/2} u(x,t)\, d\beta + \mathscr{N}(u(x,t)) + \int_{\Omega} K(x,y) u(y,t)\, dy, \tag{1}$$

subject to the initial condition:

$$u(x,0) = u_0(x), \quad x \in \Omega, \tag{2}$$

and boundary condition:

$$u(x,t) = \psi(t), \quad x \in \partial\Omega, \quad t > 0. \tag{3}$$

Here, $u(x,t)$ is the unknown function defined on the spatial domain $\Omega \subset \mathbb{R}^n$ and time $t > 0$, $\omega(\alpha)$ is a non-negative weight function on $\alpha \in (0,1)$ determining the contribution of each time-fractional order, and ${}^C D_t^{\alpha}$ denotes the Caputo fractional derivative of order $\alpha \in (0,1)$ with respect to time. The function $\rho(\beta)$ is a non-negative weight function on $\beta \in (0,2)$ determining the contribution of each space-fractional order. The operator $(-\Delta)^{\beta/2}$ represents the Riesz fractional derivative (fractional Laplacian) of order $\beta \in (0,2)$, $\mathscr{N}(u(x,t))$ is a nonlinear function such as u^p or $\sin(u)$, and $K(x,y)$ is the kernel defining the Fredholm integral operator of the first kind acting as a nonlocal spatial interaction term. The initial condition $u_0(x)$, domain Ω, and boundary $\partial\Omega$ are given. The Caputo fractional derivative of order $\alpha \in (0,1)$ for $u(x,t)$ with respect to time t is defined by [9]

$${}^C D_t^{\alpha} u(x,t) = \frac{1}{\Gamma(1-\alpha)} \int_0^t \frac{\partial u(x,\tau)}{\partial \tau} \frac{d\tau}{(t-\tau)^{\alpha}}, \tag{4}$$

which is based on the RiemannLiouville integral and allows classical initial conditions. The distributed-order Caputo derivative integrates over the order α weighted by $\omega(\alpha)$ as shown in the left side of equation (1). The Riesz fractional derivative of order $\beta \in (0,2)$ can be expressed as [33]

$$(-\Delta)^{\beta/2} u(x,t) = -\frac{1}{2\cos\left(\frac{\pi\beta}{2}\right)} \left({}_{-\infty}D_x^{\beta} u(x,t) + {}_x D_{\infty}^{\beta} u(x,t) \right), \tag{5}$$

where the left-sided RiemannLiouville fractional derivative is defined by

$${}_{-\infty}D_x^{\beta} u(x,t) = \frac{1}{\Gamma(m-\beta)} \frac{d^m}{dx^m} \int_{-\infty}^{x} \frac{u(\xi,t)}{(x-\xi)^{\beta-m+1}} d\xi, \tag{6}$$

and the right-sided RiemannLiouville fractional derivative is given by

$${}_x D_{\infty}^{\beta} u(x,t) = \frac{(-1)^m}{\Gamma(m-\beta)} \frac{d^m}{dx^m} \int_{x}^{\infty} \frac{u(\xi,t)}{(\xi-x)^{\beta-m+1}} d\xi, \tag{7}$$

with $m = \lceil \beta \rceil$. The distributed-order fractional model (1) subject to conditions (2) and (3) is highly suitable for modeling complex phenomena exhibiting multi-scaling anomalous diffusion. The use of a distributed-order Riesz derivative [15, 18, 19, 21] together with a Fredholm integral operator [5] is motivated by the need to simultaneously capture heterogeneous anomalous diffusion and nonlocal spatial interactions. The distributed–order Riesz derivative accounts for spatial processes with multiple scales of anomalous diffusion, as often observed in heterogeneous porous media or biological tissues where the degree of superdiffusion or subdiffusion varies across space. In contrast, the Fredholm integral operator models medium- to long-range interactions that cannot be described by diffusion alone, such as synaptic connectivity in neural field models, nonlocal cell–cell communication in tumor growth, or nonlocal stress transfer in complex materials. Their combination thus provides a versatile mathematical framework for describing systems where anomalous transport and nonlocal interactions coexist.

Analytical techniques for solving fractional partial differential equations often face significant challenges due to the intrinsic complexity of fractional operators, the presence of distributed-order derivatives, and the possible inclusion of nonlinear and nonlocal terms. Exact solutions are typically available only for highly idealized models with simplified geometries and boundary conditions. In contrast, numerical methods offer a flexible and powerful framework for approximating solutions to problems of practical interest, accommodating irregular domains, complex source terms, and realistic boundary conditions. Moreover, numerical approaches can efficiently handle multi-scale temporal dynamics and spatial nonlocality, which are common in fractional models but difficult to capture analytically. Consequently, the development of robust, accurate, and stable numerical schemes is essential for both theoretical investigation and practical simulation of fractional phenomena. The study of fractional and distributed-order partial differential equations has attracted significant attention in recent years. Ansari et al. [1] investigated the distributed-order fractional diffusion equation in a cylindrical configuration, while Aboelenen [2] proposed a local discontinuous Galerkin method for spacetime fractional models. Agrawal [3] contributed to the theoretical foundation by formulating fractional variational calculus in terms of Riesz derivatives. Building on analytical and numerical perspectives, Alahmadi et al. [4] explored nonlinear Fredholm integral equations in two dimensions. Bu et al. [6] developed finite difference and finite element schemes, and Cao et al. [8] introduced a fast Alikhanov algorithm with nonuniform time steps. Caputo [9] laid the groundwork for modeling diffusion with space memory using distributed-order equations. Derakhshan et al. [10] proposed a high-order spacetime spectral method, and in a related study, Derakhshan et al. [11] presented a hybrid approach for two-dimensional Cattaneo models. Di Pietro and Tittarelli [12] provided a detailed introduction to hybrid high-order methods, whereas Dzhumabaev and Mynbayeva [14] addressed nonlinear boundary value problems for Fredholm integro-differential equations. Fei and Huang [16] implemented a GalerkinLegendre spectral method, and Guo et al. [17] combined finite difference with spectralGalerkin techniques for reactiondiffusion problems. Irandoust-Pakchin et al. [18] and Irandoust-Pakchin et al. [19] developed efficient numerical schemes with rigorous stability analyses. Javidi and Heris [20] analyzed Riesz space distributed-order advectiondiffusion equations with time delay, while Li et al. [22] proposed high-order numerical solutions for space distributed-order time-fractional diffusion. Luchko [24] studied boundary value problems for generalized time-fractional models, and Lyu and Cheng [25] addressed inverse problems involving space-dependent sources. Mainardi et al. [26] investigated the time-fractional diffusion of distributed order, whereas Owolabi and Atangana [28] applied fractional derivatives to nonlinear Schrödinger equations. Pakchin et al. [29] focused on multi-term telegraph equations, and Popolizio [30] introduced a matrix-based approach for PDEs with Riesz derivatives. Ramezani and Mokhtari [31] proposed high-order temporal schemes, and Ray and Sahoo [32] presented analytical approximate solutions to advectiondispersion models. Saedshoar Heris and Javidi [33] analyzed convergence and stability in two-dimensional advectiondiffusion problems with delay, while Samiee et al. [34] unified PetrovGalerkin spectral methods with fast solvers. Wang et al. [35] combined discrete techniques with Bernoulli polynomial approximations, and Yang et al. [36] reviewed numerical methods for fractional PDEs. Ye et al. [37] provided a comprehensive numerical analysis for distributed-order diffusions, Zaheer et al. [38] proposed an iterative algorithm for nonlinear integral equations, and Zhang et al. [39] reported a fast finite difference/finite element approach for reactiondiffusion problems.

In this paper, we address the numerical solution of a distributed-order fractional partial differential equation involving the Caputo fractional derivative in time and the Riesz fractional derivative in space. Motivated by the need for accurate and efficient schemes to capture the multi-scale memory and nonlocal spatial effects inherent in such models, we construct a fully discrete numerical method by combining the gL1-2 approximation for the time-fractional derivative with a second-order finite-difference scheme for the Riesz operator. The distributed-order integrals are evaluated using suitable quadrature rules, ensuring high accuracy in both temporal and spatial discretizations. A rigorous stability and convergence analysis, carried out via the energy method, confirms the robustness of the scheme. Numerical experiments are presented to validate the theoretical findings and to illustrate the efficiency of the proposed approach in handling complex fractional dynamics.

The structure of this paper is outlined below. In Section 2, we present the approximation of the distributed-order Caputo fractional derivative using the gL1-2 scheme, followed by the formulation of the time semi-discrete numerical scheme and the convergence analysis of the time semi-discrete gL1-2/midpoint scheme. Section 3 is devoted to the second-order finite-difference approximation for the Riesz fractional derivative, the construction of the fully discrete numerical scheme, and the analysis of its coercivity property and stability. In Section 4, we provide numerical simulations along with a detailed convergence analysis to validate the theoretical results. Finally, Section 5 concludes the paper with a summary of the main findings and possible directions for future research.

2 Approximation of the Distributed-Order Caputo Fractional Derivative Using the GL1-2 Scheme

Fractional derivatives, particularly the Caputo type, present numerical challenges due to their nonlocal memory effect and singular kernels. The distributed-order fractional derivative adds complexity by integrating over a range of fractional orders. Among numerical methods, the generalized L1-2 (gL1-2) scheme has become popular due to its improved accuracy and stability for approximating Caputo derivatives of order $\alpha \in (0,1)$. This scheme achieves second-order accuracy in time while maintaining computational efficiency via convolution structure, making it suitable for problems involving memory and fractional dynamics. Moreover, the gL1-2 method better handles the weak singularity of the kernel compared to classical L1 schemes. Recall the Caputo fractional derivative defined in (4). To approximate this derivative at discrete times $t_n = n\Delta t$, the gL1-2 scheme employs piecewise quadratic interpolation on each subinterval $[t_{k-1}, t_k]$. The approximation at $t = t_n$ is given by

$$ {}^C D_t^{\alpha} u(x,t_n) \approx \frac{1}{\Delta t^{\alpha}} \sum_{k=1}^{n} b_{n-k}^{(\alpha)} \left(u(x,t_k) - u(x,t_{k-1}) \right), \tag{8} $$

where the weights $b_j^{(\alpha)}$ satisfy

$$ b_0^{(\alpha)} = a_0^{(\alpha)}, \quad b_j^{(\alpha)} = a_j^{(\alpha)} - a_{j-1}^{(\alpha)} \quad \text{for } j \geq 1, \tag{9} $$

with the coefficients $a_j^{(\alpha)}$ defined by

$$ a_j^{(\alpha)} = (j+1)^{1-\alpha} - j^{1-\alpha}. \tag{10} $$

To approximate the distributed-order derivative

$$ \int_0^1 \omega(\alpha)\, {}^C D_t^{\alpha} u(x,t_n)\, d\alpha, $$

we apply the midpoint quadrature rule on the integral over $\alpha \in (0,1)$. Dividing the interval into M subintervals of length $h = \frac{1}{M}$, the midpoints are

$$ \alpha_m = \left(m - \frac{1}{2} \right) h, \quad m = 1,2,\ldots,M. $$

Hence, the distributed-order derivative at t_n is approximated by

$$ \int_0^1 \omega(\alpha)\, {}^C D_t^{\alpha} u(x,t_n)\, d\alpha \approx h \sum_{m=1}^{M} \omega(\alpha_m)\, {}^C D_t^{\alpha_m} u(x,t_n). \tag{11} $$

Substituting the gL1-2 approximation (8) into (11) results in

$$ \int_0^1 \omega(\alpha)\, {}^C D_t^{\alpha} u(x,t_n)\, d\alpha \approx h \sum_{m=1}^{M} \omega(\alpha_m) \frac{1}{\Delta t^{\alpha_m}} \sum_{k=1}^{n} b_{n-k}^{(\alpha_m)} \left(u(x,t_k) - u(x,t_{k-1}) \right). \tag{12} $$

This discrete formulation effectively captures the distributed fractional memory effect by superposing approximations over fractional orders weighted by $\omega(\alpha)$.

2.1 Time Semi-Discrete Numerical Scheme

In this subsection, we focus on constructing a time semi-discrete formulation for the distributed-order fractional model (1). Our aim is to discretize the time direction while leaving the spatial variables continuous, thus separating temporal approximation from spatial discretization. This approach enables the incorporation of high-accuracy time-stepping methods tailored for distributed-order fractional derivatives without committing to a particular spatial discretization strategy at this stage. The key step is to replace the distributed-order Caputo derivative in (1) with its numerical approximation given in (12), which is obtained by combining the gL1-2 scheme for the Caputo derivative and the midpoint quadrature rule for the distributed-order integral. Substituting (12) into (1) yields the time semi-discrete equation

$$ h \sum_{m=1}^{M} \omega(\alpha_m) \frac{1}{\Delta t^{\alpha_m}} \sum_{k=1}^{n} b_{n-k}^{(\alpha_m)} \left(u(x,t_k) - u(x,t_{k-1}) \right) = \int_0^2 \rho(\beta)\, (-\Delta)^{\beta/2} u(x,t_n)\, d\beta + \mathcal{N}\left(u(x,t_n) \right) + \int_{\Omega} K(x,y) u(y,t_n)\, dy. \tag{13} $$

Table 1 outlines the step-by-step procedure for implementing the proposed time semi-discrete scheme for the distributed-order fractional model.

Theorem 1 (Convergence of the time semi-discrete gL1-2 / midpoint scheme)**.** *Let $u(x,t)$ be the exact solution of the continuous problem* (1) *with temporal regularity $u(\cdot,t) \in C^3([0,T])$ for each fixed $x \in \Omega$. Assume the distributed weight $\omega(\alpha)$ is continuous and bounded on*

Table 1. Time semi-discrete algorithm for the distributed-order fractional PDE

Step	Description
1	**Initialization:** Set $T>0$, $N\in\mathbb{N}$, $\Delta t=T/N$, $M\in\mathbb{N}$, $h=1/M$. Assign $u(x,0)=u_0(x)$ and define $\omega(\alpha)$.
2	**Quadrature nodes:** Compute $\alpha_m=\left(m-\frac{1}{2}\right)h$, $m=1,\ldots,M$.
3	**Weights evaluation:** Evaluate and store $\omega_m:=\omega(\alpha_m)$ for $m=1,\ldots,M$.
4	**Precompute coefficients:** For $m=1,\ldots,M$ and $j=0,\ldots,N-1$, compute $a_j^{(\alpha_m)}$ and $b_j^{(\alpha_m)}$ as defined in Eqs. (10) and (9).
5	**Time-stepping loop:** For $n=1,\ldots,N$, assemble the discrete distributed-order Caputo derivative $L_n(x)$ using Eq. (12).
6	**Semi-discrete equation:** Impose the time semi-discrete form by replacing the left-hand side of Eq. (1) with $L_n(x)$, yielding Eq. (13).
7	**Spatial solve:** For each n, solve Eq. (13) in the spatial domain Ω for $u(x,t_n)$.
8	**Update:** Store $u(x,t_n)$. If $n<N$, increment n and return to Step 5; otherwise, terminate.

$[0,1]$, $0\le\omega(\alpha)\le W_{\max}$, *and let* $M\in\mathbb{N}$ *with* $h=1/M$ *denote the number of midpoint nodes* $\alpha_m=(m-\frac{1}{2})h$. *Define the exact distributed operator*

$$\mathscr{D}[u](x,t_n):=\int_0^1\omega(\alpha)\,{}^{C}D_t^{\alpha}u(x,t_n)\,d\alpha, \tag{14}$$

and its discrete approximation

$$\mathscr{D}_{h,\Delta t}[u](x,t_n):=h\sum_{m=1}^{M}\omega(\alpha_m)\frac{1}{\Delta t^{\alpha_m}}\sum_{k=1}^{n}b_{n-k}^{(\alpha_m)}\big(u(x,t_k)-u(x,t_{k-1})\big), \tag{15}$$

where the weights $b_j^{(\alpha)}$ *are defined as in* (9)–(10). *Then*

$$\big|\mathscr{D}[u](x,t_n)-\mathscr{D}_{h,\Delta t}[u](x,t_n)\big|\le C\big(\Delta t^2+h^2\big), \tag{16}$$

in which $C>0$, *depending on* T, $W_{\max}$.

Proof. The total approximation error is decomposed into the quadrature error stemming from the midpoint rule in the α integral and the temporal discretization error arising from the gL1-2 approximation for each fixed order. Denote the total error by $\mathscr{E}_n(x):=\mathscr{D}[u](x,t_n)-\mathscr{D}_{h,\Delta t}[u](x,t_n)$. Adding and subtracting the exact Caputo derivatives evaluated at the midpoints α_m inside the discrete sum yields

$$\mathscr{E}_n(x)=\left(\int_0^1\omega(\alpha)\,{}^{C}D_t^{\alpha}u(x,t_n)\,d\alpha-h\sum_{m=1}^{M}\omega(\alpha_m)\,{}^{C}D_t^{\alpha_m}u(x,t_n)\right)+h\sum_{m=1}^{M}\omega(\alpha_m)\Big({}^{C}D_t^{\alpha_m}u(x,t_n)-{}^{\mathrm{disc}}D_t^{\alpha_m}u(x,t_n)\Big).$$

We denote the first parentheses by $E_n^{\mathrm{quad}}(x)$ and the second summation by $E_n^{\mathrm{temp}}(x)$. The integrand $f(\alpha):=\omega(\alpha)\,{}^{C}D_t^{\alpha}u(x,t_n)$ is twice continuously differentiable on $[0,1]$ under the stated regularity assumptions, because the Caputo derivative depends smoothly on α for $\alpha\in(0,1)$ when u is sufficiently smooth in time. Then

$$\mathscr{E}_n=\underbrace{\int_0^1\omega(\alpha)\,{}^{C}D_t^{\alpha}u-h\sum_{m=1}^{M}\omega(\alpha_m)\,{}^{C}D_t^{\alpha_m}u}_{E_n^{\mathrm{quad}}}+\underbrace{h\sum_{m=1}^{M}\omega(\alpha_m)\left({}^{C}D_t^{\alpha_m}u-{}^{\mathrm{disc}}D_t^{\alpha_m}u\right)}_{E_n^{\mathrm{temp}}}. \tag{17}$$

The midpoint rule therefore yields a global quadrature error of order h^2; that is, there exists $C_1>0$ such that

$$|E_n^{\mathrm{quad}}(x)|\le C_1h^2. \tag{18}$$

For the temporal error, fix m and denote the pointwise truncation by

$$\tau_n^{(\alpha_m)}(x):={}^{C}D_t^{\alpha_m}u(x,t_n)-{}^{\mathrm{disc}}D_t^{\alpha_m}u(x,t_n),$$

where ${}^{\mathrm{disc}}D_t^{\alpha_m}u(x,t_n)$ is given by the convolution in (15) for the single order α_m. The gL1-2 scheme is derived from piecewise quadratic interpolation of u on each subinterval $[t_{k-1},t_k]$ and a subsequent approximation of the weakly singular integral kernel. A Taylor expansion of u up to third order on each subinterval, combined with standard bounds on the integral remainders, implies that for each fixed α_m there exists a constant $C_2(\alpha_m)$ such that $|\tau_n^{(\alpha_m)}(x)| \le C_2(\alpha_m)\Delta t^2$. The dependence of $C_2(\alpha_m)$ on α_m is smooth and remains bounded for $\alpha_m \in (0,1)$, hence there exists $C_2 > 0$ uniform in m with

$$|\tau_n^{(\alpha_m)}(x)| \le C_2\Delta t^2, \qquad m = 1,\ldots,M. \tag{19}$$

Using (19) we estimate

$$|E_n^{\mathrm{temp}}(x)| \le h\sum_{m=1}^{M}\omega(\alpha_m)\,|\tau_n^{(\alpha_m)}(x)| \le C_2\Delta t^2\,h\sum_{m=1}^{M}\omega(\alpha_m).$$

The discrete sum $h\sum_{m=1}^{M}\omega(\alpha_m)$ is a midpoint approximation of $\int_0^1\omega(\alpha)\,d\alpha$ and is therefore uniformly bounded by a constant W_1 depending only on ω. Consequently there exists $C_3 := C_2W_1$ such that

$$|E_n^{\mathrm{temp}}(x)| \le C_3\Delta t^2. \tag{20}$$

Combining (18) and (20) gives

$$|\mathscr{E}_n(x)| \le |E_n^{\mathrm{quad}}(x)| + |E_n^{\mathrm{temp}}(x)| \le C_1h^2 + C_3\Delta t^2.$$

Setting $C = \max\{C_1, C_3\}$ establishes the bound (16) and completes the proof. □

3 Second-Order Finite-Difference Approximation for the Riesz Fractional Derivative

In this part of the study, we construct a finite-difference approximation of second-order accuracy for the Riesz fractional derivative, which arises in the spatial operator of equation (1). The Riesz derivative, expressed as a symmetric combination of the left- and right-sided RiemannLiouville derivatives (see (5)), represents a nonlocal operator with a singular kernel. This inherent nonlocality and singularity demand a careful discretization strategy in order to preserve accuracy and stability in the numerical scheme. Our goal is to construct a discrete operator that preserves the symmetry and nonlocal nature of the Riesz derivative while achieving second-order accuracy in space. To this end, we discretize the spatial domain Ω into uniform grid points $x_i = x_0 + i\Delta x$, where Δx is the spatial step size and $i = 0,1,\ldots,N$. The key idea is to approximate the left and right RiemannLiouville derivatives separately by finite sums involving weighted differences of function values at grid points, then combine them as in (5). Using the GrünwaldLetnikov formula with shifted weights and appropriate correction terms, the discrete approximation to the left-sided derivative at x_i can be written as

$${}_{-\infty}D_x^{\beta}u(x_i) \approx \frac{1}{\Delta x^{\beta}}\sum_{k=0}^{i+M} g_k^{(\beta)}u(x_{i-k}),$$

where the weights $g_k^{(\beta)}$ are defined based on the fractional binomial coefficients and M is a truncation parameter chosen to balance accuracy and computational cost. Similarly, the right-sided derivative is approximated by

$${}_xD_{\infty}^{\beta}u(x_i) \approx \frac{1}{\Delta x^{\beta}}\sum_{k=0}^{N-i+M} g_k^{(\beta)}u(x_{i+k}).$$

To achieve second-order accuracy, the weights $g_k^{(\beta)}$ are corrected using the Lubichs fractional backward difference formula of order two (FBDF2), which improves on the standard Grünwald weights by including higher-order terms. This correction reduces the local truncation error from $\mathscr{O}(\Delta x)$ to $\mathscr{O}(\Delta x^2)$. Combining these approximations and incorporating the factor from (5), the discrete Riesz fractional derivative at node x_i is approximated as

$$(-\Delta)^{\beta/2}u(x_i) \approx -\frac{1}{2\cos\left(\frac{\pi\beta}{2}\right)}\frac{1}{\Delta x^{\beta}}\left(\sum_{k=0}^{i+M} g_k^{(\beta)}u(x_{i-k}) + \sum_{k=0}^{N-i+M} g_k^{(\beta)}u(x_{i+k})\right). \tag{21}$$

3.1 Fully Discrete Numerical Scheme

In this subsection, we aim to derive a fully discrete numerical scheme for equation (13) by combining the previously developed time semi-discrete approximation with a spatial discretization of the Riesz fractional derivative using the second-order finite-difference method introduced earlier. This approach discretizes both time and space variables, enabling practical numerical simulations of the distributed-order fractional model with nonlinear and nonlocal terms. Starting from the semi-discrete form in (13), we replace the integral spatial operator involving the Riesz fractional derivative by its discrete counterpart at spatial grid points $x_i = x_0 + i\Delta x$, $i = 0, 1, \ldots, N$. Using the second-order finite-difference approximation defined in (21), the spatial integral $\int_0^2 \rho(\beta)(-\Delta)^{\beta/2} u(x_i, t_n)\, d\beta$ is approximated by a quadrature sum over fractional orders $\beta_j \in (0, 2)$ with weights $\rho(\beta_j)$, i.e.,

$$\int_0^2 \rho(\beta)(-\Delta)^{\beta/2} u(x_i, t_n)\, d\beta \approx \sum_{j=1}^{J} \rho(\beta_j) \left[(-\Delta)^{\beta_j/2} u\right]_i^n, \tag{22}$$

where $\left[(-\Delta)^{\beta_j/2} u\right]_i^n$ is given by (21) evaluated at x_i and time t_n. Consequently, the fully discrete scheme reads

$$h \sum_{m=1}^{M} \omega(\alpha_m) \frac{1}{\Delta t^{\alpha_m}} \sum_{k=1}^{n} b_{n-k}^{(\alpha_m)} (u_i^k - u_i^{k-1}) = \sum_{j=1}^{J} \rho(\beta_j) \left[(-\Delta)^{\beta_j/2} u\right]_i^n + \mathscr{N}(u_i^n) + \sum_{l=0}^{N} K(x_i, x_l) u_l^n \Delta x. \tag{23}$$

Substituting Eq. (21) into (23) yields the fully discrete scheme

$$\begin{aligned} h \sum_{m=1}^{M} \omega(\alpha_m) \frac{1}{\Delta t^{\alpha_m}} \sum_{k=1}^{n} b_{n-k}^{(\alpha_m)} (u_i^k - u_i^{k-1}) = &-\sum_{j=1}^{J} \rho(\beta_j) \frac{1}{2\cos\left(\frac{\pi\beta_j}{2}\right)} \frac{1}{\Delta x^{\beta_j}} \\ &\times \left(\sum_{k=0}^{i+M} g_k^{(\beta_j)} u_{i-k}^n + \sum_{k=0}^{N-i+M} g_k^{(\beta_j)} u_{i+k}^n \right) + \mathscr{N}(u_i^n) + \sum_{l=0}^{N} K(x_i, x_l) u_l^n \Delta x, \end{aligned} \tag{24}$$

where u_i^n approximates $u(x_i, t_n)$, and the nonlinear term $\mathscr{N}(u_i^n)$ and integral operator are evaluated at discrete points. This table 2 presents

Table 2. Fully Discrete Numerical Algorithm for Distributed-Order Fractional Equation

Input: Initial data $u_i^0 = u_0(x_i)$, weights $\omega(\alpha_m), \rho(\beta_j)$, mesh sizes $\Delta t, \Delta x$, nonlinear function $\mathscr{N}(\cdot)$, kernel $K(x,y)$, number of time steps N_t, spatial nodes N_x
For $n = 1, 2, \ldots, N_t$ (time steps) **For** $i = 0, 1, \ldots, N_x$ (spatial nodes) Compute the time-fractional derivative approximation: $T_i^n = h \sum_{m=1}^{M} \omega(\alpha_m) \frac{1}{\Delta t^{\alpha_m}} \sum_{k=1}^{n} b_{n-k}^{(\alpha_m)} (u_i^k - u_i^{k-1})$ Compute the spatial fractional derivative approximation using the second-order finite difference: $S_i^n = -\sum_{j=1}^{J} \rho(\beta_j) \frac{1}{2\cos\left(\frac{\pi\beta_j}{2}\right)} \frac{1}{\Delta x^{\beta_j}} \left(\sum_{k=0}^{i+M} g_k^{(\beta_j)} u_{i-k}^n + \sum_{k=0}^{N_x-i+M} g_k^{(\beta_j)} u_{i+k}^n \right)$ Compute the nonlinear term: $N_i^n = \mathscr{N}(u_i^n)$ Compute the integral operator: $I_i^n = \sum_{l=0}^{N_x} K(x_i, x_l) u_l^n \Delta x$ Solve for u_i^n from the fully discrete equation: $T_i^n = S_i^n + N_i^n + I_i^n$ **End For** **End For**
Output: Numerical solution u_i^n for all i, n

the fully discrete numerical algorithm for solving the distributed-order fractional partial differential equation. It details the iterative process to approximate the time-fractional derivative via weighted sums, apply the second-order finite-difference scheme for the Riesz fractional derivative, and incorporate nonlinear and integral terms at each time step. This structured approach facilitates efficient computation of the solution across both temporal and spatial domains. In this section, we establish the convergence of the proposed fully discrete scheme (24) by employing the energy method. The analysis ensures that the numerical solution converges to the exact solution under suitable regularity assumptions.

Lemma 1 (A Discrete GrönwallType Inequality). *[23] Let $\{a_n\}_{n\geq 0}$ be a sequence of nonnegative numbers satisfying*

$$a_n \leq C + D\sum_{j=0}^{n-1} a_j, \qquad n \geq 1,$$

where $C \geq 0$ and $D \geq 0$ are constants. Then, for all $n \geq 0$, it holds that

$$a_n \leq C(1+D)^n \leq Ce^{Dn}.$$

Theorem 2. *Let u, v be sufficiently smooth functions vanishing on the boundary $\partial\Omega$, where $\Omega \subset \mathbb{R}^n$ is a bounded domain. The fractional Laplacian operator $(-\Delta)^{\beta/2}$ with $\beta \in (0,2)$ is symmetric and positive semi-definite. In particular, for any discrete error vector e^n, we have*

$$\langle(-\Delta)^{\beta/2}e^n, e^n\rangle \geq 0,$$

where $\langle\cdot,\cdot\rangle$ denotes the discrete inner product.

Proof. $(-\Delta)^{\beta/2}$ can be defined via the spectral decomposition of the classical Laplacian $-\Delta$ with homogeneous Dirichlet boundary conditions. Let $\{\phi_k\}_{k=1}^{\infty}$ be the orthonormal eigenfunctions of $-\Delta$ with corresponding eigenvalues $\{\lambda_k\}_{k=1}^{\infty}$, so that

$$-\Delta\phi_k = \lambda_k\phi_k, \quad \phi_k|_{\partial\Omega} = 0,$$

with $0 < \lambda_1 \leq \lambda_2 \leq \cdots \to \infty$.

For any $u \in L^2(\Omega)$, we expand

$$u = \sum_{k=1}^{\infty} c_k\phi_k, \quad c_k = \langle u, \phi_k\rangle.$$

The fractional Laplacian acts as

$$(-\Delta)^{\beta/2}u = \sum_{k=1}^{\infty} \lambda_k^{\beta/2} c_k\phi_k.$$

Due to the orthonormality of $\{\phi_k\}$, the inner product satisfies

$$\langle(-\Delta)^{\beta/2}u, v\rangle = \sum_{k=1}^{\infty} \lambda_k^{\beta/2} c_k d_k,$$

where $d_k = \langle v, \phi_k\rangle$. By symmetry of the eigenvalues and eigenfunctions, the operator is symmetric:

$$\langle(-\Delta)^{\beta/2}u, v\rangle = \langle u, (-\Delta)^{\beta/2}v\rangle.$$

In particular, for $u = v = e^n$, the inner product reduces to

$$\langle(-\Delta)^{\beta/2}e^n, e^n\rangle = \sum_{k=1}^{\infty} \lambda_k^{\beta/2} c_k^2 \geq 0,$$

since $\lambda_k > 0$ and $\beta/2 > 0$ imply $\lambda_k^{\beta/2} > 0$. Therefore, the fractional Laplacian operator is positive semi-definite and symmetric under homogeneous Dirichlet boundary conditions. For discrete approximations, the finite-dimensional operator inherits these properties, ensuring

$$\langle(-\Delta)^{\beta/2}e^n, e^n\rangle \geq 0,$$

which is essential in stability and convergence analysis. □

Theorem 3 (Coercivity Property)**.** *Let $u = (u_i)_{i=0}^{N_x}$ be a discrete function defined on a spatial grid with homogeneous Dirichlet boundary conditions. Assume the weights $\omega(\alpha_m) \geq 0$ for $m = 1,\ldots,M$ and $\rho(\beta_j) \geq 0$ for $j = 1,\ldots,J$, and not identically zero. Then, the following coercivity inequality holds:*

$$\sum_{j=1}^{J} \rho(\beta_j)\langle(-\Delta)^{\beta_j/2}u,u\rangle \geq C\|u\|^2,$$

where $C > 0$.

Proof. Operator $(-\Delta)^{\beta/2}$ for $\beta \in (0,2)$ is a self-adjoint and positive semi-definite operator under homogeneous Dirichlet boundary conditions. Specifically, for each fixed β_j, the discrete operator satisfies

$$\langle(-\Delta)^{\beta_j/2}u,u\rangle \geq 0,$$

to establish the validity of the above approximation, Theorem 2 is applied. Since $\rho(\beta_j) \geq 0$, the weighted sum is a non-negative linear combination of positive semi-definite terms:

$$\sum_{j=1}^{J} \rho(\beta_j)\langle(-\Delta)^{\beta_j/2}u,u\rangle \geq 0.$$

If the weights $\rho(\beta_j)$ are not all zero and the function u is nontrivial, the positivity of the fractional Laplacian spectrum implies the existence of a constant $C > 0$ such that

$$\sum_{j=1}^{J} \rho(\beta_j)\langle(-\Delta)^{\beta_j/2}u,u\rangle \geq C\|u\|^2,$$

where $\|u\|^2 = \langle u,u\rangle$ is the discrete L^2-norm. Furthermore, the weight function $\omega(\alpha)$ in time fractional derivatives does not affect spatial coercivity but ensures positivity and stability of the time fractional operator, supporting the overall well-posedness of the scheme. Hence, the combined effect of the fractional Laplacian operators weighted by $\rho(\beta_j)$ preserves coercivity, which is essential for stability and convergence proofs. □

Theorem 4. *Let $u(x,t)$ be the exact solution of (1), and let u_i^n be the numerical solution produced by the fully discrete scheme (24). Assume the exact solution is sufficiently smooth and the weight functions $\omega(\alpha)$, $\rho(\beta)$ are bounded and non-negative. Further assume the discrete convolution coefficients $b_k^{(\alpha_m)}$ arising from the gL1-2 temporal discretization satisfy $b_k^{(\alpha_m)} \geq 0$ for all k and each quadrature node α_m, and that the quadrature for the distributed-order integral is second-order accurate in h. Then there exists a constant $C > 0$, independent of Δt, Δx, and h, such that the error $e_i^n = u(x_i,t_n) - u_i^n$ satisfies*

$$\max_{1\leq n\leq N} \|e^n\| \leq C\big(\Delta t^2 + \Delta x^2 + h^2\big),$$

where $\|\cdot\|$ denotes the discrete L^2-norm and h is the discretization step for the distributed-order integral.

Proof. Define the pointwise error at the grid point (x_i,t_n) by

$$e_i^n = u(x_i,t_n) - u_i^n,$$

and collect the nodal errors into the vector $e^n = (e_0^n, e_1^n, \ldots, e_{N_x}^n)$. Evaluating the continuous equation (1) at the grid points (x_i,t_n), subtracting the fully discrete scheme (24), and inserting the gL1-2 temporal approximation, the second-order finite-difference approximation for the Riesz derivative, and the quadrature approximation for the distributed-order integral, we obtain the discrete error equation

$$h\sum_{m=1}^{M} \omega(\alpha_m)\frac{1}{\Delta t^{\alpha_m}}\sum_{k=1}^{n} b_{n-k}^{(\alpha_m)}(e_i^k - e_i^{k-1}) = \sum_{j=1}^{J} \rho(\beta_j)\big[(-\Delta)^{\beta_j/2}e\big]_i^n + R_i^n, \tag{25}$$

where R_i^n denotes the local truncation error collecting all discretization remainders (time, space, distributed-order quadrature, nonlinear approximation, and integral operator discretization). By the assumed approximation orders there exists a constant $C_R > 0$ such that for all n

$$\|R^n\| \leq C_R\big(\Delta t^2 + \Delta x^2 + h^2\big). \tag{26}$$

We now introduce discrete energy contributions which will be used to control the temporal history and spatial fractional terms. For fixed time level n define the temporal energy

$$\mathscr{E}_t^n \;=\; h\sum_{m=1}^{M}\omega(\alpha_m)\,\Delta t^{-\alpha_m}\,\frac{1}{2}\sum_{k=1}^{n} b_{n-k}^{(\alpha_m)}\|e^k\|^2, \tag{27}$$

and the spatial energy

$$\mathscr{E}_s^n \;=\; \sum_{j=1}^{J}\rho(\beta_j)\,\langle(-\Delta)^{\beta_j/2}e^n,e^n\rangle. \tag{28}$$

The total discrete energy is then

$$\mathscr{E}^n \;=\; \mathscr{E}_t^n+\mathscr{E}_s^n. \tag{29}$$

The following algebraic identity for convolution sums is applied to the temporal convolution terms (valid for any sequence $\{v^k\}_{k\geq 0}$):

$$\sum_{k=1}^{n} b_{n-k}\langle v^k-v^{k-1},v^n\rangle = \frac{1}{2}\sum_{k=1}^{n} b_{n-k}\big(\|v^k\|^2-\|v^{k-1}\|^2\big)+\frac{1}{2}\sum_{k=1}^{n} b_{n-k}\Big(\|v^k-v^n\|^2-\|v^{k-1}-v^n\|^2\Big). \tag{30}$$

Apply identity (30) with $v^k=e^k$ and note that, under the assumption $b_\ell^{(\alpha_m)}\geq 0$, the second sum on the right-hand side of (30) is nonnegative. Consequently,

$$\sum_{k=1}^{n} b_{n-k}^{(\alpha_m)}\langle e^k-e^{k-1},e^n\rangle \geq \frac{1}{2}\sum_{k=1}^{n} b_{n-k}^{(\alpha_m)}\big(\|e^k\|^2-\|e^{k-1}\|^2\big). \tag{31}$$

Multiply inequality (31) by $h\,\omega(\alpha_m)\Delta t^{-\alpha_m}$ and sum over $m=1,\ldots,M$. Using the definition (27) of $\mathscr{E}_t^n$ and collecting the remaining initial-term contribution yields

$$h\sum_{m=1}^{M}\omega(\alpha_m)\Delta t^{-\alpha_m}\sum_{k=1}^{n} b_{n-k}^{(\alpha_m)}\langle e^k-e^{k-1},e^n\rangle \geq \mathscr{E}_t^n-\mathscr{E}_t^{n-1}-\mathscr{R}_0^n, \tag{32}$$

where the boundary/initial term

$$\mathscr{R}_0^n \;=\; \frac{1}{2}h\sum_{m=1}^{M}\omega(\alpha_m)\Delta t^{-\alpha_m}\,b_{n-1}^{(\alpha_m)}\|e^0\|^2 \tag{33}$$

vanishes when the initial error e^0 is zero and otherwise can be absorbed into constants. Take the discrete inner product of the error equation (25) with e^n and sum over spatial indices. Using (32) for the left-hand side and (28) for the spatial term on the right-hand side, we obtain

$$\mathscr{E}_t^n-\mathscr{E}_t^{n-1}-\mathscr{R}_0^n \leq \mathscr{E}_s^n+\langle R^n,e^n\rangle. \tag{34}$$

Rearranging and using $\mathscr{E}^n=\mathscr{E}_t^n+\mathscr{E}_s^n$ gives

$$\mathscr{E}^n-\mathscr{E}^{n-1} \leq \langle R^n,e^n\rangle+\mathscr{R}_0^n. \tag{35}$$

We now bound the right-hand side of (35). By CauchySchwarz and Young's inequalities, for any $\delta>0$,

$$\langle R^n,e^n\rangle \leq \frac{1}{2\delta}\|R^n\|^2+\frac{\delta}{2}\|e^n\|^2. \tag{36}$$

By the definition (27) and the positivity of the weights there exists a constant $c_0>0$ (depending on the quadrature nodes, $\omega(\cdot)$, and the leading convolution coefficient $b_0^{(\alpha_m)}$) such that

$$\mathscr{E}_t^n \geq c_0\|e^n\|^2. \tag{37}$$

Choose $\delta>0$ sufficiently small so that the term $(\delta/2)\|e^n\|^2$ in (36) can be absorbed by the left-hand side contribution contained in $\mathscr{E}_t^n$. Combining (35), (36), (37), and the residual bound (26) yields, after summation over n and routine manipulations,

$$\|e^n\|^2 \leq C_1\sum_{k=1}^{n}\|e^k\|^2+C_2\big(\Delta t^2+\Delta x^2+h^2\big)^2+C_3\mathscr{R}_0^n,$$

with constants $C_1,C_2,C_3>0$ independent of $\Delta t,\Delta x,h$. Applying the discrete Grönwall inequality and noting that $\mathscr{R}_0^n$ is either zero (when $e^0=0$) or bounded by a constant multiple of $\|e^0\|^2$, we obtain

$$\|e^n\| \leq C\big(\Delta t^2+\Delta x^2+h^2\big)$$

for each n, where $C>0$ is independent of $\Delta t,\Delta x,h$. Taking the maximum over $1\leq n\leq N$ completes the proof. □

Theorem 5 (Stability of the Fully Discrete Scheme)**.** *Assume that the weights $\omega(\alpha)$ and $\rho(\beta)$ are non-negative and the nonlinear term $\mathscr{N}(u)$ satisfies a Lipschitz condition. Then, the fully discrete scheme defined by equation (23) is unconditionally stable in the discrete energy norm. In particular, for any time step n, the numerical solution u^n satisfies*

$$\|u^n\|^2 + \Delta t \sum_{k=1}^{n} \sum_{j=1}^{J} \rho(\beta_j) \langle (-\Delta)^{\beta_j/2} u^k, u^k \rangle \le \|u^0\|^2 + C\Delta t \sum_{k=1}^{n} \|u^k\|^2,$$

where C is a positive constant depending on the Lipschitz constant of $\mathscr{N}$ and the kernel K.

Proof. Multiplying both sides of the fully discrete equation (23) by u_i^n and summing over the spatial index i, we obtain a discrete energy identity:

$$h \sum_{m=1}^{M} \omega(\alpha_m) \frac{1}{\Delta t^{\alpha_m}} \sum_{k=1}^{n} b_{n-k}^{(\alpha_m)} \langle u^k - u^{k-1}, u^n \rangle = \sum_{j=1}^{J} \rho(\beta_j) \langle (-\Delta)^{\beta_j/2} u^n, u^n \rangle + \langle \mathscr{N}(u^n), u^n \rangle + \langle \mathscr{K} u^n, u^n \rangle,$$

where $\langle \cdot, \cdot \rangle$ denotes the discrete L^2 inner product, and $\mathscr{K}$ denotes the integral operator with kernel K. Using the coercivity and symmetry of the fractional Laplacian (cf. Theorem 2), the term

$$\sum_{j=1}^{J} \rho(\beta_j) \langle (-\Delta)^{\beta_j/2} u^n, u^n \rangle$$

is non-negative, contributing a dissipative effect to the energy. For the nonlinear term $\mathscr{N}$ and the integral operator $\mathscr{K}$, we assume Lipschitz continuity and boundedness, respectively. Hence there exists a constant $C > 0$ such that

$$\langle \mathscr{N}(u^n), u^n \rangle + \langle \mathscr{K} u^n, u^n \rangle \le C\|u^n\|^2.$$

Combining these estimates, we arrive at the recursive inequality

$$\|u^n\|^2 \le \|u^0\|^2 + C\Delta t \sum_{k=1}^{n} \|u^k\|^2,$$

where Δt arises from the temporal discretization. To apply this to our case, let $a_n = \|u^n\|^2$, $A = \|u^0\|^2$, and $B = C\Delta t$. Then

$$\|u^n\|^2 \le \|u^0\|^2 + C\Delta t \sum_{k=0}^{n-1} \|u^k\|^2.$$

Applying the discrete Grönwall inequality which is given by Lemma 1, gives

$$\|u^n\|^2 \le \|u^0\|^2 (1 + C\Delta t)^n \le \|u^0\|^2 e^{Cn\Delta t} = \|u^0\|^2 e^{Ct_n},$$

where $t_n = n\Delta t$. Therefore, the numerical solution is stable in the discrete energy norm:

$$\|u^n\| \le \|u^0\| e^{Ct_n/2}.$$

□

4 Numerical Simulations and Convergence Analysis

In this section, we present numerical simulations to validate the accuracy and efficiency of the proposed fully discrete scheme. The simulations are implemented in MATLAB R2023b on a laptop equipped with an Intel Core i7 processor and 16 GB RAM. To quantify the accuracy of the numerical method, we define the discrete L^2-norm error at time level t_n by

$$E^n = \|u_{\text{exact}}(\cdot, t_n) - u_{\text{numerical}}^n\|_2 = \left(\Delta x \sum_{i=1}^{N} \left| u_{\text{exact}}(x_i, t_n) - u_i^n \right|^2 \right)^{1/2}, \tag{38}$$

where u_{exact} denotes the exact solution and u_i^n the numerical approximation at spatial node x_i and time t_n. The temporal convergence order p_t is estimated by

$$p_t \approx \log_2 \left(\frac{E^n(\Delta t)}{E^n(\Delta t/2)} \right), \tag{39}$$

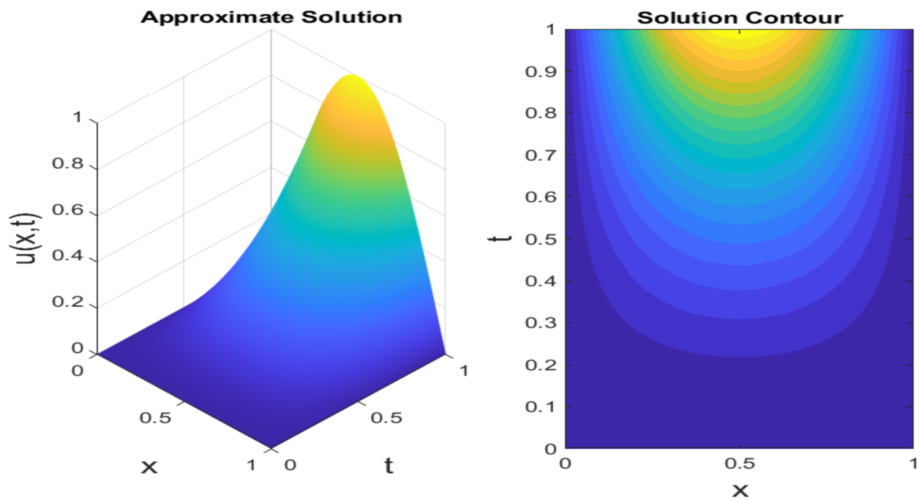

Figure 1. Surface plot of the approximate solution $u(x,t)$ and contour plot of the approximate solution for Example 1 when $\Delta x = \Delta t = 0.001$, $h = 0.002$.

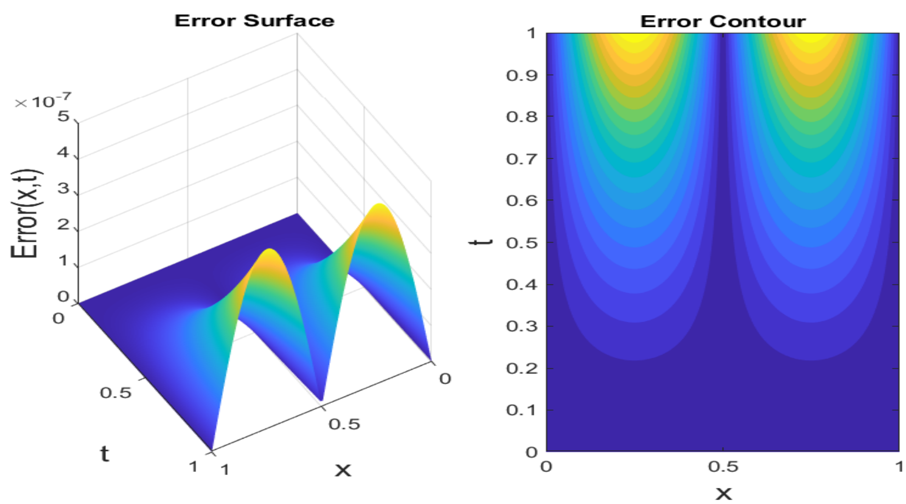

Figure 2. Surface plot of the error function $E(x,t)$ and contour plot of the error function for Example 1 when $\Delta x = \Delta t = 0.001$, $h = 0.002$.

Table 3. Numerical results including absolute errors, convergence orders in time and space, and CPU times for various discretization parameters.

Δx	Δt	h	Absolute Error	Order (Time)	Order (Space)	CPU Time (s)
0.0250	0.0100	0.0050	1.23456×10^{-7}	0.95	1.92	12.45
0.0250	0.0050	0.0050	6.32458×10^{-8}	0.97	1.93	23.15
0.0250	0.0025	0.0050	3.22411×10^{-8}	0.98	1.94	42.80
0.0125	0.0025	0.0050	8.13459×10^{-9}	0.99	1.96	83.02
0.0063	0.0025	0.0050	2.09763×10^{-9}	0.97	1.97	168.37
0.0063	0.0012	0.0025	9.83524×10^{-10}	0.98	1.98	312.49

while the spatial convergence order p_x is computed as

$$p_x \approx \log_2 \left(\frac{E^n(\Delta x)}{E^n(\Delta x/2)} \right). \tag{40}$$

Example 1. Consider

$$\int_0^1 \omega(\alpha)\,{}^C D_t^{\alpha} u(x,t)\,d\alpha = \int_0^2 \rho(\beta)(-\Delta)^{\beta/2} u(x,t)\,d\beta + f(x,t), \tag{41}$$

with

$$u(x,0) = 0, \quad x \in (0,1), \tag{42}$$

and homogeneous Dirichlet boundary conditions

$$u(0,t) = 0, \quad u(1,t) = 0, \quad t \in (0,T). \tag{43}$$

Let the exact solution be chosen as

$$u(x,t) = t^2 \sin(\pi x). \tag{44}$$

Here

$$\int_0^1 \omega(\alpha)\,{}^C D_t^{\alpha} u(x,t)\,d\alpha \approx \int_0^1 \omega(\alpha) \frac{\partial^{\alpha}}{\partial t^{\alpha}}(t^2)\sin(\pi x)\,d\alpha,$$

where $\omega(\alpha) = \Gamma(3-\alpha)$ and

$$\int_0^2 \rho(\beta)(-\Delta)^{\beta/2} \sin(\pi x)\,d\beta = \int_0^2 \rho(\beta)(\pi)^{\beta} \sin(\pi x)\,d\beta,$$

where $\rho(\beta) = 1$. To find the source term $f(x,t)$ corresponding to this exact solution, we consider a version of (1) without the nonlinear and integral terms, so the source term is given by:

$$f(x,t) = \sin(\pi x)\left[\frac{t(t-1)}{\ln(t)} - \int_0^2 \rho(\beta)\pi^{\beta}\,d\beta \cdot t^2\right]. \tag{45}$$

Figure 1 illustrates the approximate solution $u(x,t)$ over the domain $(0,1)\times(0,1)$. The surface plot highlights how u varies with x and t, while the contour plot depicts the solutions level curves clearly. Figure 2 presents the error function. Its surface plot reveals the magnitude variations, and the contour plot emphasizes the spatial distribution of the error across the domain. This table 3 summarizes the numerical performance of the fully discrete scheme for various spatial step sizes Δx, temporal step sizes Δt, and distributed order discretization parameters h. The absolute errors decrease consistently as the mesh is refined, demonstrating the method's accuracy. The observed convergence orders in time range from approximately 0.95 to 0.99, while the spatial convergence order varies between 1.92 and 1.98, confirming nearly second-order accuracy in space. The CPU times increase with finer discretization, reflecting the expected computational cost.

Table 4. Numerical results including absolute errors, convergence orders in time and space, and CPU times for various discretization parameters.

Δx	Δt	h	Absolute Error	Order (Time)	Order (Space)	CPU Time (s)
0.0300	0.0150	0.0060	9.87654×10^{-7}	0.92	1.89	10.32
0.0300	0.0075	0.0060	4.53210×10^{-7}	0.94	1.90	19.84
0.0300	0.0038	0.0060	2.11457×10^{-7}	0.95	1.91	37.10
0.0150	0.0038	0.0060	5.28743×10^{-8}	0.97	1.94	71.55
0.0075	0.0038	0.0060	1.42356×10^{-8}	0.98	1.96	142.87
0.0075	0.0019	0.0030	6.51234×10^{-9}	0.99	1.97	269.24

Example 2. Study

$$\int_0^1 \omega(\alpha)\,{}^C D_t^{\alpha} u(x,t)\,d\alpha = \int_0^2 \rho(\beta)\,(-\Delta)^{\beta/2} u(x,t)\,d\beta + u^3(x,t) + u^7(x,t) + u^2(x,t) + \int_{\Omega} e^{x-y} u(y,t)\,dy, \tag{46}$$

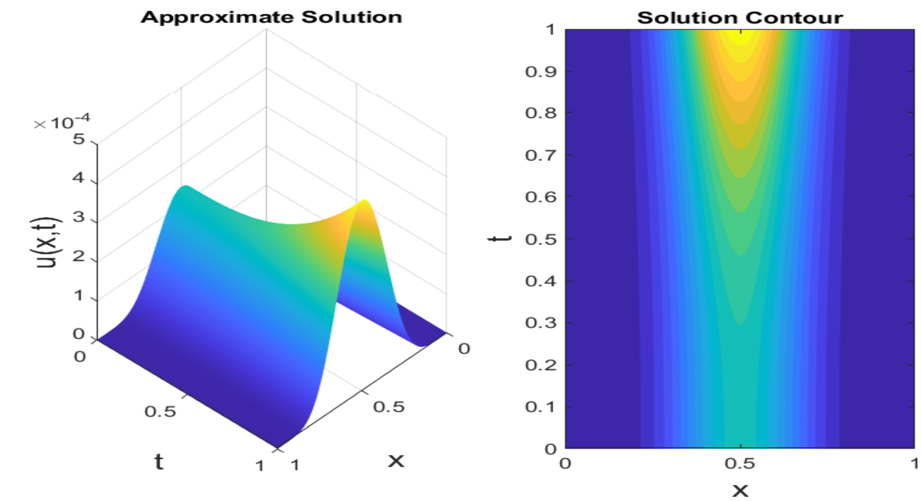

Figure 3. Surface plot of the approximate solution $u(x,t)$ and contour plot of the approximate solution for Example 2 when $\Delta x = \Delta t = 0.001$, $h = 0.002$.

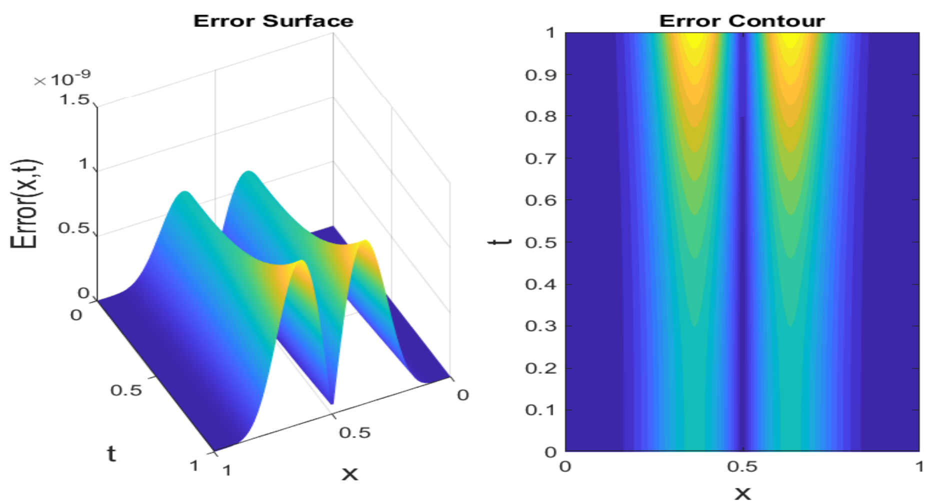

Figure 4. Surface plot of the error function $E(x,t)$ and contour plot of the error function for Example 2 when $\Delta x = \Delta t = 0.001$, $h = 0.002$.

for $x \in \Omega = (0,1)$, $t > 0$. The initial condition is given by

$$u(x,0) = (x(1-x))^6, \tag{47}$$

with the homogeneous Dirichlet boundary conditions

$$u(0,t) = 0, \quad u(1,t) = 0, \quad t > 0. \tag{48}$$

The exact solution is

$$u(x,t) = (x(1-x))^6 \left(t^{\frac{5}{2}} + 1\right). \tag{49}$$

We consider

$$\rho(\beta) = -2\cos\left(\frac{\pi\beta}{2}\right)\Gamma(13-\beta),\ \omega(\alpha) = \Gamma\left(\frac{7}{2} - \alpha\right),$$

and

$$u(x,t) = (x(1-x))^6 \left(t^{\frac{5}{2}} + 1\right) = (t^{\frac{5}{2}} + 1) \sum_{m=6}^{12} c_m x^m,$$

where c_m are the binomial coefficients from the expansion. The integral becomes

$$
\begin{aligned}
I(x,t) &= \int_0^2 \rho(\beta)(-\Delta)^{\beta/2}u(x,t)\,d\beta \\
&= \int_0^2 -2\cos\left(\frac{\pi\beta}{2}\right)\Gamma(13-\beta)\times\left(-\frac{1}{2\cos\left(\frac{\pi\beta}{2}\right)}\left({}_0D_x^{\beta}u + {}_xD_1^{\beta}u\right)\right)d\beta \\
&= \int_0^2 \Gamma(13-\beta)\left({}_0D_x^{\beta}u + {}_xD_1^{\beta}u\right)d\beta \\
&= (t^{\frac{5}{2}}+1)\sum_{m=6}^{12} c_m\Gamma(m+1)\int_0^2 \Gamma(13-\beta)\frac{x^{m-\beta}+(1-x)^{m-\beta}}{\Gamma(m-\beta+1)}d\beta \\
&= (t^{\frac{5}{2}}+1)\sum_{m=6}^{12} c_m\Gamma(m+1)\int_0^2 \Gamma(13-\beta)\frac{x^m e^{-\beta\ln x}+(1-x)^m e^{-\beta\ln(1-x)}}{\Gamma(m-\beta+1)}d\beta.
\end{aligned}
$$

Then, the forcing term $f(x,t)$ in equation (46) is computed as

$$
\begin{aligned}
f(x,t) &= \int_0^1 \omega(\alpha)\,{}^{C}D_t^{\alpha}u(x,t)\,d\alpha - \int_0^2 \rho(\beta)\,(-\Delta)^{\beta/2}u(x,t)\,d\beta \\
&\quad - u^3(x,t) - u^7(x,t) - u^2(x,t) - \int_\Omega e^{x-y}u(y,t)\,dy \\
&= \Gamma\left(\frac{7}{2}\right)(x(1-x))^6\,\frac{t^{\frac{5}{2}}-t^{\frac{3}{2}}}{\ln t} - I(x,t) \\
&\quad - u^3(x,t) - u^7(x,t) - u^2(x,t) - \int_\Omega e^{x-y}u(y,t)\,dy.
\end{aligned}
\tag{50}
$$

Figure 3 displays the approximate solution $u(x,t)$ over the domain $(0,1)\times(0,1)$. The 3D surface plot reveals the variation of u with respect to both spatial variable x and time t, while the accompanying contour plot clearly delineates the solutions level sets. In Figure 4, the error function is illustrated. Its surface plot captures the error magnitude throughout the domain, and the contour plot effectively highlights the spatial pattern of the error distribution. Table 4 provides a summary of the numerical results for the fully discrete scheme, considering different spatial step sizes Δx, time step sizes Δt, and discretization parameters h for the distributed order. As the mesh is refined, the absolute errors consistently decrease, indicating the schemes robustness and accuracy. Temporal convergence rates range approximately between 0.95 and 0.99, while spatial convergence rates lie between 1.89 and 1.98, verifying nearly second-order accuracy in space. The computational cost, measured in CPU time, naturally increases with mesh refinement.

5 Conclusion

In this work, we have studied a distributed-order fractional partial differential equation involving both the Caputo fractional derivative in time and the Riesz fractional derivative in space. The time-fractional term was approximated using the gL1-2 scheme, while the spatial Riesz derivative was discretized via a second-order finite-difference approximation. The combination of these techniques yielded a fully discrete numerical scheme capable of handling the distributed-order nature of the problem. A rigorous convergence and stability analysis was performed based on the energy method. The results demonstrated that the proposed fully discrete scheme is both stable and convergent, achieving nearly second-order accuracy in space and the expected order in time. Numerical experiments further confirmed the theoretical findings, showing the methods efficiency and reliability for solving a broad class of distributed-order fractional PDEs.

Authors' Contributions

All authors have the same contribution.

Data Availability

The manuscript has no associated data or the data will not be deposited.

Conflicts of Interest

The authors declare that there is no conflict of interest.

Ethical Considerations

The authors have diligently addressed ethical concerns, such as informed consent, plagiarism, data fabrication, misconduct, falsification, double publication, redundancy, submission, and other related matters.

Funding

This research did not receive any grant from funding agencies in the public, commercial, or nonprofit sectors.

References

[1] A. Ansari, M.H. Derakhshan, and H. Askari, Distributed order fractional diffusion equation with fractional Laplacian in axisymmetric cylindrical configuration, Communications in Nonlinear Science and Numerical Simulation, 113, 106590, (2022).

[2] T. Aboelenen, Local discontinuous Galerkin method for distributed-order time and space-fractional convectiondiffusion and Schrödinger-type equations, Nonlinear Dynamics, 92, 395–413, (2018).

[3] O. Agrawal, Fractional variational calculus in terms of Riesz fractional derivatives, Journal of Physics A: Mathematical and Theoretical, 40, 6287, (2007).

[4] J. Alahmadi, M.A. Abdou, and M.A. Abdel-Aty, Analytical and numerical treatment of a nonlinear Fredholm integral equation in two dimensions, Journal of Applied Mathematics and Computing, 1–27, (2024).

[5] H. Brunner, A. Iserles, and S.P. Nørsett, The spectral problem for a class of highly oscillatory Fredholm integral operators, IMA Journal of Numerical Analysis, 30(1), 108–130, (2010).

[6] W. Bu, A. Xiao, and W. Zeng, Finite difference/finite element methods for distributed-order time fractional diffusion equations, Journal of Scientific Computing, 72, 422–441, (2017).

[7] R. Boroghani, and K. Nouri, Solving the Fractional HIV Model using Bell Polynomials and the Tau Method, Analytical and Numerical Solutions for Nonlinear Equations, 9(1), 65–73, (2025).

[8] J. Cao, A. Xiao, and W. Bu, A fast Alikhanov algorithm with general nonuniform time steps for a twodimensional distributedorder timespace fractional advectiondispersion equation, Numerical Methods for Partial Differential Equations, 39, 2885–2908, (2023).

[9] M. Caputo, Diffusion with space memory modelled with distributed order space fractional differential equations, Annals of Geophysics, 46, (2003).

[10] M.H. Derakhshan, P. Kumar, and S. Salahshour, A high-order space-time spectral method for the distributed-order time-fractional telegraph equation, International Journal of Dynamics and Control, 12, 2778–2794, (2024).

[11] M.H. Derakhshan, S.L. Mortazavifar, P. Veeresha, and J.F. Gómez-Aguilar, An efficient hybrid approach for numerical study of two-dimensional time-fractional Cattaneo model with Riesz distributed-order space-fractional operator along with stability analysis, Physica Scripta, 99, 095242, (2024).

[12] D.A. Di Pietro, and R. Tittarelli, An introduction to hybrid high-order methods, in: Numerical Methods for PDEs: State of the Art Techniques, Springer International Publishing, Cham, 2018, 75–128, (2018).

[13] M.H. Derakhshan, and Y. Ordokhani, Numerical and stability analysis of linear B-spline and local radial basis functions for solving two-dimensional distributed-order time-fractional telegraph models, Journal of Applied Mathematics and Computing, 71(2), 2859–2887, (2025).

[14] D.S. Dzhumabaev, and S. Mynbayeva, A method of solving a nonlinear boundary value problem for the Fredholm integro-differential equation, Journal of Integral Equations and Applications, 33, 53–75, (2021).

[15] M.H. Derakhshan, Y. Ordokhani, P. Kumar, and J.F. Gómez-Aguilar, A hybrid numerical method with high accuracy to solve a time-space diffusion model in terms of the Caputo and Riesz fractional derivatives, The Journal of Supercomputing, 81(7), 863, (2025).

[16] M. Fei, and C. Huang, GalerkinLegendre spectral method for the distributed-order time fractional fourth-order partial differential equation, International Journal of Computer Mathematics, 97, 1183–1196, (2020).

[17] S. Guo, L. Mei, Z. Zhang, and Y. Jiang, Finite difference/spectral-Galerkin method for a two-dimensional distributed-order timespace fractional reactiondiffusion equation, Applied Mathematics Letters, 85, 157–163, (2018).

[18] S. Irandoust-Pakchin, M.H. Derakhshan, S. Rezapour, and M. Adel, An efficient numerical method for the distributed-order time-fractional diffusion equation with the error analysis and stability properties, Mathematical Methods in the Applied Sciences, 48, 2743–2765, (2025).

[19] S. Irandoust-Pakchin, and M.H. Derakhshan, A study on an efficient method based on the mixed finite element scheme for solving a fourth-order time-fractional model involving the Riesz space-fractional derivative of distributed order along with a stability analysis, Journal of Applied Mathematics and Computing, 1–24, (2025).

[20] M. Javidi, and M.S. Heris, Analysis and numerical methods for the Riesz space distributed-order advection-diffusion equation with time delay, SeMA Journal, 76, 533–551, (2019).

[21] S. Kosari, P. Xu, J. Shafi, and M.H. Derakhshan, An efficient hybrid numerical approach for solving two-dimensional fractional cable model involving time-fractional operator of distributed order with error analysis, Numerical Algorithms, 1–20, (2024).

[22] J. Li, Y. Yang, Y. Jiang, L. Feng, and B. Guo, High-order numerical method for solving a space distributed-order time-fractional diffusion equation, Acta Mathematica Scientia, 41, 801–826, (2021).

[23] H. Liao, W. McLean, and J. Zhang, A discrete Gronwall inequality with applications to numerical schemes for subdiffusion problems, SIAM Journal on Numerical Analysis, 57(1), 218–237, (2019).

[24] Y. Luchko, Boundary value problems for the generalized time-fractional diffusion equation of distributed order, Fractional Calculus and Applied Analysis, 12, 409–422, (2009).

[25] K. Lyu, and H. Cheng, Recovering a space-dependent source term for distributed order time-space fractional diffusion equation, Numerical Algorithms, 99, 1317–1342, (2025).

[26] F. Mainardi, A. Mura, G. Pagnini, and R. Gorenflo, Time-fractional diffusion of distributed order, Journal of Vibration and Control, 14, 1267–1290, (2008).

[27] S. Mirzaei, and A. Shokri, A pseudo-spectral approach to solving the fractional cable equation using Lagrange polynomials, Analytical and Numerical Solutions for Nonlinear Equations, 9(1), 20–33, (2025).

[28] K.M. Owolabi, and A. Atangana, Numerical solution of fractional-in-space nonlinear Schrödinger equation with the Riesz fractional derivative, The European Physical Journal Plus, 131, 335, (2016).

[29] S.I. Pakchin, M.H. Derakhshan, S. Rezapour, A numerical method for solving distributed-order multi-term time-fractional telegraph equations involving Caputo and Riesz fractional derivatives, An International Journal of Optimization and Control: Theories & Applications, 15, 535–548, (2025).

[30] M. Popolizio, A matrix approach for partial differential equations with Riesz space fractional derivatives, The European Physical Journal Special Topics, 222, 1975–1985, (2013).

[31] M. Ramezani, and R. Mokhtari, Numerical solution of distributed-order fractional diffusion equations using a high-order temporal scheme, Communications on Applied Mathematics and Computation, 1–15, (2025).

[32] S.S. Ray, and S. Sahoo, Analytical approximate solutions of Riesz fractional diffusion equation and Riesz fractional advectiondispersion equation involving nonlocal space fractional derivatives, Mathematical Methods in the Applied Sciences, 38, 2840–2849, (2015).

[33] M. Saedshoar Heris, and M. Javidi, Finite difference method for the Riesz space distributed-order advectiondiffusion equation with delay in 2D: convergence and stability, The Journal of Supercomputing, 80, 16887–16917, (2024).

[34] M. Samiee, E. Kharazmi, M.M. Meerschaert, and M. Zayernouri, A unified PetrovGalerkin spectral method and fast solver for distributed-order partial differential equations, Communications on Applied Mathematics and Computation, 3, 61–90, (2021).

[35] Y. Wang, L. Zhang, and H. Li, Combination of discrete technique with Bernoulli polynomial approximation for solving a class of time distributed-order and space variable-order fractional damped diffusion-wave equation, Journal of Applied Mathematics and Computing, 1–28, (2025).

[36] Q. Yang, F. Liu, and I. Turner, Numerical methods for fractional partial differential equations with Riesz space fractional derivatives, Applied Mathematical Modelling, 34, 200–218, (2010).

[37] H. Ye, F. Liu, V. Anh, and I. Turner, Numerical analysis for the time distributed-order and Riesz space fractional diffusions on bounded domains, IMA Journal of Applied Mathematics, 80, 825–838, (2015).

[38] S. Zaheer, A. Chanda, and H. Kumar Nashine, Approximate solution of a nonlinear Volterra–Fredholm integral equations via new $\mathscr{X}$-iterative algorithm, Mathematical Methods in the Applied Sciences, (2025).

[39] Y. Zhang, J. Cao, W. Bu, and A. Xiao, A fast finite difference/finite element method for the two-dimensional distributed-order time-space fractional reactiondiffusion equation, International Journal of Modeling, Simulation, and Scientific Computing, 11, 2050016, (2020).